
Article:
Patacci, M orcid.org/0000-0003-1675-4643, Marini, M, Felletti, F et al. (3 more authors) (2020) Origin of mud in turbidites and hybrid event beds: Insight from ponded mudstone caps of the Castagnola turbidite system (north-west Italy). Sedimentology, 67 (5). pp. 2625-2644. ISSN 0037-0746

https://doi.org/10.1111/sed.12713

Accepted for publication on Sedimentology on 17 January 2020

Origin of mud in turbidites and hybrid event beds: insight from ponded mudstone caps of the Castagnola turbidite system (NW Italy)

Marco Patacci[1] (*), Mattia Marini[2], Fabrizio Felletti[2], Andrea Di Giulio[3], Massimo Setti[3], William McCaffrey[1]

[1] School of Earth and Environment, University of Leeds, Leeds, UK

[2] Dipartimento di Scienze della Terra, Università degli Studi di Milano, Milano, Italy

[3] Dipartimento di Scienze della Terra e dell'Ambiente, Università degli Studi di Pavia, Pavia, Italy

(*) corresponding author: M.Patacci@leeds.ac.uk

Abstract

The partitioning of different grain size classes in gravity flow deposits is one of the key characteristics used to infer depositional processes. Turbidites have relatively clean sandstones with most of their clay deposited as part of a mudstone cap or as a distal mudstone layer, whereas sand-bearing debrites commonly comprise mixtures of sand grains and interstitial clay; hybrid event beds develop alternations of clean and dirty (clay-rich) sandstones in varying proportions. Analysis of co-genetic mudstone caps in terms of thickness and composition is a novel approach that can provide new insight into gravity flow depositional processes. Bed thickness data from the ponded Castagnola system show that turbidites contain more clay overall than do hybrid event beds. The Castagnola system is characterised by deposits of two very different petrographic types. Thanks to this duality, analyses of sandstone and mudstones composition allow inference of which proportion of the clay in both deposit types was acquired en-route. In combination with standard sedimentological observations the new data allow insight into the likely characteristics of their parent flows. Clean turbidites were deposited

by lower concentration, long duration, erosive, muddy turbidity currents which were more efficient at fractionating clay particles away from their basal layer. Hybrid event beds were deposited by shorter duration, higher-concentration, less-erosive sandier flows which were less efficient at clay fractionation. The results are consistent with data from other turbidite systems (e.g., Marnoso-arenacea). The approach represents a new method to infer the controls on the degree of clay partitioning in gravity flow deposits.

Keywords: turbidite; hybrid event bed; ponding; bed thickness; mudstone cap; mudcap

1. Introduction

One of the key challenges in understanding particulate gravity flows is being able to predict the distance they can travel and how far they can deposit the different grain size classes they transport (Talling et al., 2015). This is a complex, non-linear problem related to the properties of the substrate (slope angle, grain size and mechanical properties) and to those of the flow (duration, mass flux, grain size distribution of the transported sediment, rheology; Meiburg and Kneller, 2010; Dorrell at al., 2018). A common approach is to use the concept of 'flow efficiency' (*sensu* Mutti and Normark, 1987). In this type of analysis, flow volume and grain size of the transported particles are highlighted as major controls on the distance flows can travel and on the resulting deposit geometry (Mutti et al., 1999). In particular, the amount of mud carried by a flow is considered key to its sand transport efficiency, i.e., its ability to deposit sand far from the entry point into the depositional system (Gladstone et al., 1998; Al Ja'Aidi et al., 2004). The effects of clay particles in gravity flows include providing long-lasting flow bulking (i.e., clay particles increase excess density of the flow while having a very low settling rate) and modifications to the flow behaviour (turbulent, transitional or laminar; e.g., Baas et al 2009). However, increasing clay proportions only increases efficiency up to a threshold, above which clay cohesion suppresses turbulence and hinders the flow ability to move downstream, with different types of clay resulting in different threshold values (e.g., Baker et al., 2017). Flows may fail to reach this threshold concentration if enough clay particles are fractionated (i.e. differentially segregated) from the main body of the flow and mixed with ambient water.

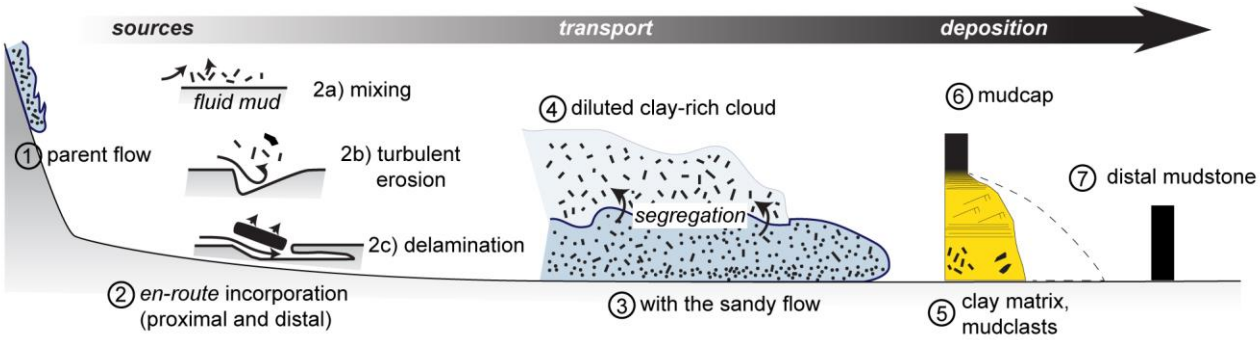

Figure 1: Clay in sandy gravity flows (dots: sand; dashes: clay; black shapes: clay clasts). The sketch illustrates the sources of clay (parent flow, en-route incorporation), its transport (as part of a sand-bearing flow or as a diluted clay-rich cloud following segregation) and finally its deposition within the 'sandy' bed (clay matrix and/or mudclasts), above it (mudstone cap) or distally (mudstone layer). No downstream distance scale implied.

A second key challenge is to develop a better understanding of the degree to which sand and mud are segregated in the deposit and what controls the deposition of matrix-poor vs matrix-rich sandstones. This has been the subject of much research in the last fifteen years focusing on the occurrence and distribution of hybrid event beds (i.e. turbiditic event beds with a matrix- or intraclast-rich division; Haughton et al., 2009; Talling, 2013; Fonnesu et al., 2018).

For both these challenges, the amount, type and distribution of clay particles in the flow remains key to understanding flow behaviour and deposit character (see Fig. 1 for a summary of the sources, sinks and associated processes affecting clay particles in mixed sand-mud gravity flows). Despite this, most sedimentological research has focussed on the sandy deposit, for both practical and applied reasons. Sandstone layers have better outcrop expression, provide a wealth of sedimentary structures that can be observed in the field and can more easily be linked to flow events. Additionally, sandstones receive special consideration because of their applied significance, because their porous nature enables them to act as reservoirs, for example for water or hydrocarbons (e.g., Weimer and Slatt, 2007).

While there has been significant work in looking at the amount and significance of clay locked into sandstone beds as interstitial clay or as mudstone clasts (e.g., Ito, 2008; Porten et al, 2016; Bell et al., 2018; Angus et al., 2019), mudstone caps (e.g., Sagri, 1979) and distal mudstones (e.g., Pierce et al., 2018; Boulesteix et al., 2019) are relatively understudied, although they often represent the

deposit of the bulk of the clay transported by turbidity currents and hybrid flows. Reasons for the paucity of studies include poor exposure and the apparently monotonous nature of muddy successions, which make it challenging to distinguish individual events in the field and to correlate them to their more proximal sand-mud couplet counterparts; rare examples include a thin muddy deposit correlated 100s of km away from the pinch-out of the sand in the offshore NW Africa (Georgiopoulou et al., 2009). One solution to this issue is to look at events that are fully ponded, which make the link between sandstone and their associated mudstones clearer, because of the special geometry of their deposits.

In this paper “full ponding” is used to indicate events for which both the sandy and muddy parts of the flow were interacting with and fully contained within a bathymetric low (c.f. Van Andel and Komar 1969; Toniolo et al., 2007; Patacci et al., 2015). Note that this definition refers to single depositional events, as in the same depocentre events with different volume or flow type might experience different degrees of ponding. From this definition, it follows that in a confined depocentre a fully ponded flow event will leave a sandy deposit generally overlain by a thicker than normal muddy deposit (see Haughton, 1994; 2000), with the two having roughly the same area (i.e. sand reaches the edges of the basin and mud is not stripped downstream). In other words, the event has no distal associated mudstone and all the mud is deposited either within the sandstone bed or above it, making up its mudstone cap. In this scenario, it becomes possible to estimate the total volume of the sandstone and mudstone from measured sedimentary logs (e.g., see Sumner et al., 2012). For this study, thickness data from fully ponded sandstone and mudstone co-genetic couplets (i.e. event beds) from the Castagnola turbidite system were used, and the results compared with published data on fully and partially ponded events from the Marnoso-Arenacea Formation (Malgesini et al., 2015 and Sumner et al., 2012).

The principal aim of this paper is to gain insight into mechanisms and volumes of clay acquisition and segregation during transport, and on their control on the resulting deposit. Specific research objectives include:

a) recognition of mudstone caps co-genetic with different types of sandy gravity flow deposits (e.g., turbidites and hybrid event beds) and their thickness with relation to that of the sandstone deposit;
b) characterization of the composition and provenance of sandstones and their co-genetic mudstone caps to allow insight into clay sources and entrainment mechanisms.

2. Geological setting

2.1 Castagnola turbidite system

The Castagnola turbidite system is part of the Aquitanian-Burdigalian sedimentary fill of the eastern portion of the Tertiary Piedmont Basin (TPB) of NW Italy, an episutural basin located above the junction between the Western Alps and the Northern Apennines (Fig. 2A; for more details on the TPB see Mosca et al., 2010; Maino et al., 2013). The paleogeography of the eastern part of the TPB at the time of the deposition of the Castagnola system was characterised by a narrow shelf with fan deltas to the south, the Monferrato high to the W-SW and by the transpressive Villalvernia-Varzi line to the north dividing it from the foreland (Rossi et al., 2009; Rossi and Craig, 2016; Fig. 2B). Areas where sediments correlative to the Castagnola system are limited or missing suggest the presence of a number of local intrabasinal highs (Andreoni et al., 1981). The palaeotopography of this portion of the TPB was therefore likely characterised by a number of tortuous corridors or possibly by a chain of small minibasins (Marini et al., 2016A), rather than that of a single larger sub-basin.

The outcrops of the Castagnola syncline (Andreoni et al., 1981; Baruffini et al., 1994) allow insight into a relatively distal part of the turbidite system (c. 30-40 km from the contemporaneous shelf; Fig. 2B), deposited against a NE-SW striking confining slope running along the Villalvernia-Varzi line (see inferred key bed terminations against the slope in Fig. 2C). Palaeocurrent indicators suggest that flows reached this area from the south and that they were deflected by the confining slope toward the east (Cavanna et al., 1989; Felletti et al., 2002; Southern et al., 2015). The study area includes the easternmost and therefore more distal outcrops of the Castagnola turbidite system, but due to later uplift and erosion it is unclear how further down-dip the system extended. In the Castagnola syncline,

sedimentary facies, architecture and bed thicknesses indicate a transition from a lower ponded succession with thick mudstone caps to an upper unconfined depositional environment (Costa Grande and Arenaceo Members; Marini et al., 2016A). The sketch logs shown in Fig. 2D illustrate the tabular nature (thinning rate of 0.15-0.05 m/Km for beds 0.3-1.5 m thick; Tőkés and Patacci, 2018) of the lower 600 m thick ponded sequence (up to key bed 400; Unit 1 of Marini et al., 2016A). Above key bed 400, Marini et al., 2016A recognise a c. 100 m thick transitional unit interpreted as confined with respect to the sand, but not to the muds (their Unit 2) followed by a >200 m thick unit (their Unit 3) characterised by compensational architectures and interpreted as being unconfined (only the lowermost part is shown in Fig. 2D).

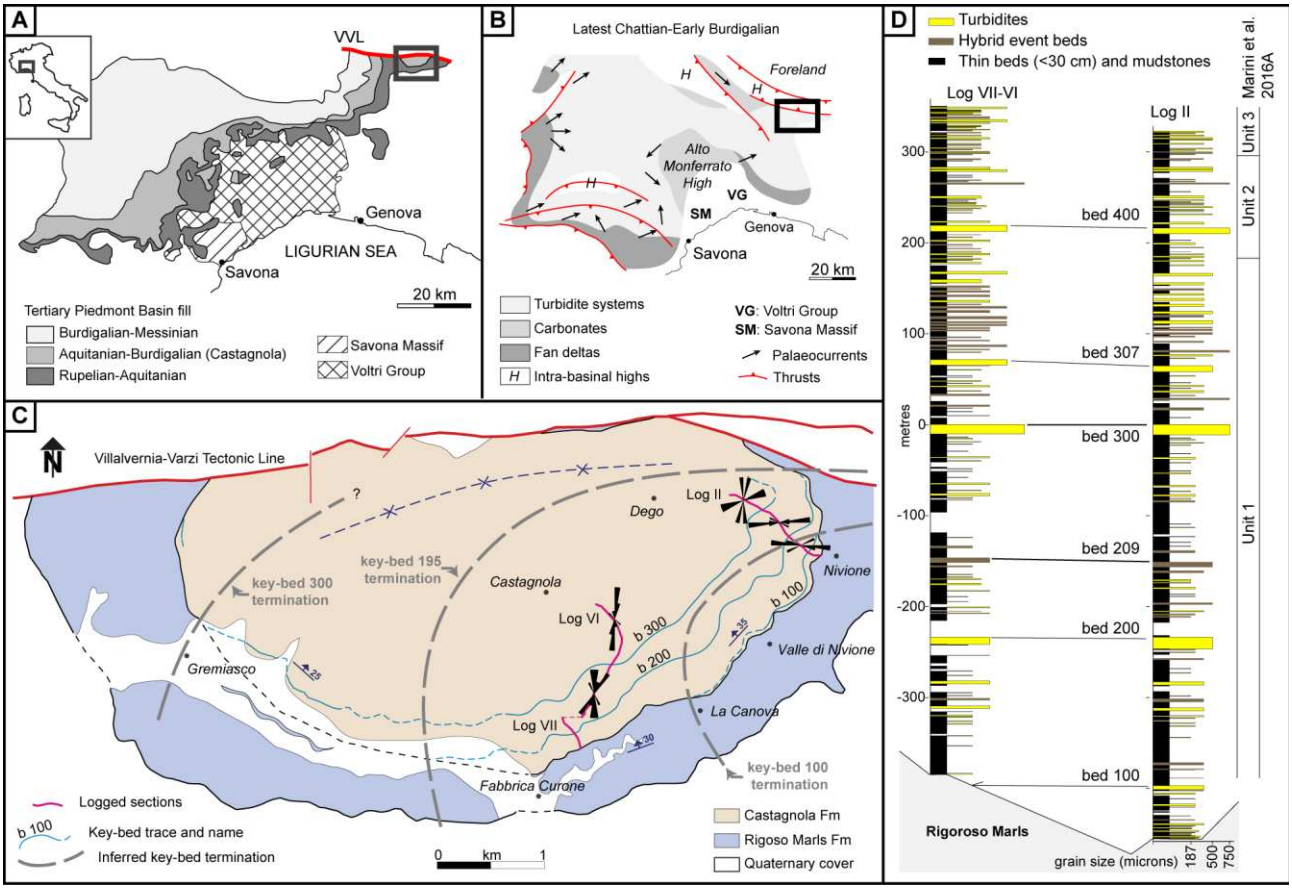

Figure 2. A) Location and simplified geological map of the Tertiary Piedmont Basin fill (modified from Mutti et al., 2002, Mosca et al., 2010). VVL: Villalvernia-Varzi Tectonic Line. B) Palaeogeographic map at the Chattian-Burdigalian boundary time (modified from Rossi et al., 2009). Location of southern sediment sources (Savona Massif and Voltri Group) is highlighted. C) Geological map of the Castagnola syncline (black boxes in parts A and B); formation boundaries and structure after Cavanna et al., 1989. Trace of key sandstone beds (dashed light blue) and their inferred subsurface terminations (dashed grey), based on mapped onlap relationships. Measured logs trace and palaeocurrents (from sole structures), divided per stratigraphic interval (base-bed 200, bed 200-bed

300 and bed 300-top); rare directional sole structures indicate flow toward north and east. D) Synthetic sedimentary log panel (only beds >29 cm are shown); see part C for logs location (pink lines). Full log panel is available as part of the supplementary material.

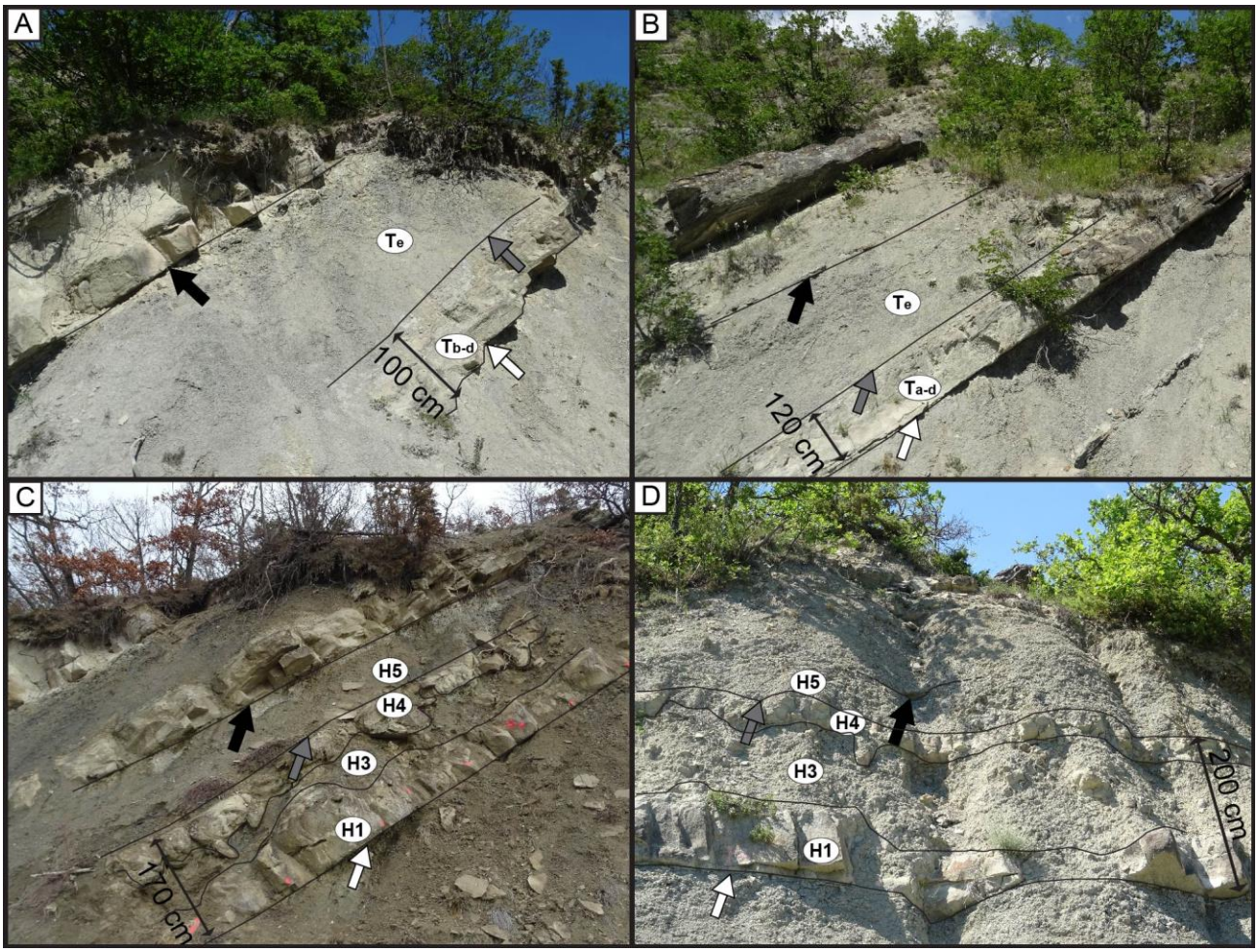

Figure 3. Examples of turbidites (A-B) and hybrid event beds (C-D) characteristic of the Castagnola turbidite system. Arrows indicate: bed base (white), sandstone bed top (grey), mudstone cap top (black). Labels indicate Bouma divisions for turbidites (Bouma, 1962) and H divisions for hybrid event beds (Haughton et al., 2009). Note that Te corresponds to H5 (mudstone cap associated with the gravity flow).

The ponded interval between bed 100 and bed 400 has a low net-to-gross of c. 0.3 (log II) and it is characterised by four main bed types, with grain size ranging from fine to medium sand and occasionally up to coarse (see Southern et al., 2015 and Marini et al., 2016A for detailed sedimentological descriptions):

1) megabeds, here defined as having a sandstone layer thicker than 6 metres (type A of Southern et al., 2015 and Marini et al., 2016A);

2) turbidites, made up of complete or base-missing graded Bouma sequences and tops often characterised by bedform sets with opposite palaeocurrent directions (type B of Southern et al., 2015 and Marini et al., 2016A);
3) hybrid event beds, characterised by a chaotic middle division enriched in clay matrix or mudstone clasts sandwiched between a lower structureless sandstone division and an upper rippled and/or parallel-laminated sandstone division (type C of Southern et al., 2015 and Marini et al., 2016A);
4) thin beds, here defined as having a sandstone layer thinner than 30 cm (type D of Southern et al., 2015 and Marini et al., 2016A).

This study compares turbidites (Fig. 3A-B) and hybrid event beds (Fig. 3C-D), which in the ponded interval between bed 100 and bed 400 represent 35% and 30% of the sandstone thickness, respectively. The exclusion of megabeds and thin beds was based on a number of methodological and sedimentological considerations (more details below), including number of samples available (small for megabeds), grain size (too fine for quantitative thin section analysis for thin beds), and ponding degree and bed geometry (thin beds were likely not fully ponded and more lenticular, according to the ponding definition above).

Published data on sandstone petrography (Cibin et al., 2003) show that the beds in the ponded interval of the Castagnola Formation have sandstone compositions that fall into discrete categories. Most are either ophiolite-rich lithic or arkosic in character; a much smaller proportion is of mixed lithic-arkosic composition. This compositional division suggests that at initiation the parent flows might have been sourced by completely different parent rocks exposed in two (possibly neighbouring) drainage areas. It follows that the mud carried by these flows at initiation might also have had distinct mineralogy, mirroring that of the associated sands. If so, it might be possible to distinguish mud carried by the initial flow from the mud incorporated en-route.

3. Methodology

This study makes combined use of three datasets: a) sandstone and mudstones thicknesses for each event bed, b) sandstone petrography and c) mudstone mineralogy.

3.1 Thickness data

Measuring sandstone and their associated mudstone thicknesses was performed as part of a detailed sedimentological logging exercise (Log VII-VI and Log II; see Fig. 2C-D). Measurements were undertaken using a high-precision Jacob's staff with laser (Patacci, 2016) to minimise measurement error, particularly that associated with sighting in the common scenario of logging along crest tops where bed dips and outcrop slopes are similar (see Fig. 4).

Figure 4. Measuring mudstone caps with a high-precision Jacob's staff (Patacci, 2016). A trowel is used to keep the staff steady at the base of the sandstone bed. The bright dot (white arrow) projected on the outcrop by the rotating laser follows the bed base, aiding sighting. The laser beam cannot be seen in daylight and has been added digitally.

In addition, accurate measurement of sandstone and mudstone intervals for each event bed at one location required careful consideration of the geometry and position of the three defining surfaces

(base of sandstone, top of sandstone/base of mudstone cap and top of mudstone cap; for hybrid beds, the top of the sandstone layer is taken as the top of the H4 division). In general, the geometry of these surfaces is planar and parallel to structural tilt at the outcrop scale (tens of metres; and indeed at much greater scale, as log correlation illustrates; see Fig. 2D). However, while determining the position of the base of the sandstone is generally straightforward, an accurate determination of the other two requires a consistent logging methodology. The top of the siltstone/base of the mudstone cap was determined in the field by sampling and comparing by visual observation and by touch; hence, although the exact transition point chosen could be considered arbitrary, consistency is expected to be high. Although the siltstone was included as part of the sandstone layer, the mudcaps also contain minor proportions of silt-sized particles. The top of the mudstone cap can be difficult to determine accurately where it is overlain by an unrelated silty or muddy layer. Few occurrences of cm-thick hemipelagites can be distinguished thanks to their less micaceous composition, biogenic content (foraminiferal and radiolaria tests) and lighter colour. In other cases, the transition from the clayey top of a mudcap to the base of the next event can be detected because of an abrupt increase in silt. Great care was taken in the field to clean the outcrops to highlight such subtle changes in colour and texture of the mudstone. In addition, in some instances when it was possible to identify a feature (e.g. mm-thin siltstone or sandstone layer) delimiting the mudcap top only on one of the two correlated logs, the values on the log where the feature could not be identified were not included in the analysis. Another factor affecting the measured thickness is erosion by later events; however, this issue is thought to be relatively minor, as the larger events object of this study (sandstone thickness >29 cm) are usually overlain by thin beds (sandstone thickness <30 cm), which do not show evidence of erosion in the study area.

Finally, it should be noted that the measurements taken in the field do not represent the original values at the time of deposition, because of compaction. Decompaction has not been considered in this study because its inclusion would not affect the findings and for ease of comparison with other datasets, as other authors commonly do not include decompaction in their analysis.

3.2 Sandstone petrography data

Samples from sandstone beds were collected a few centimetres above bed bases, avoiding any basal coarser lag or heavily weathered intervals. Petrography was determined by optical microscope modal analysis. A point counting was performed on each sample according to the method described in Cibin et al. (2004), considering all rock constituents (essential and accessory framework grains, matrix, cements) and counting at least 250 essential grains (Q-F-L grains). The Gazzi-Dickinson method of counting (based on considering all sand-sized components as separate grains, regardless of what they are connected to) was used in order to minimize the effect of sample grain size on classification parameters (e.g., Ingersoll et al., 1984). Therefore, in the following the term lithic grains refers to fine-grained rock fragments only, i.e. polymineralic grains made by constituents smaller than 0.062 mm. The dataset consists of 59 beds with a sandstone division thicker than 29 cm (47 turbidites and 12 hybrid event beds. The sampled beds represent roughly half of the beds with a sandstone division thicker than 29 cm in the interval between bed 93 and bed 433 (see Log panel in the supporting information for the detailed position of all sampled beds). The full dataset is presented in the supplementary material.

3.3 Mudstone composition data

Samples for mudstone composition analysis were collected from the mid-point of the mudstone cap for consistency and to avoid the risk of sampling outside of the mudstone cap itself (as might happen sampling near the top) or of taking samples with a considerable silt fraction (as might happen sampling the base). The dataset comprises 47 samples from beds with a sandstone division thicker than 29 cm (39 turbidites and 8 hybrid event beds) and 6 from thinner beds. Overall, 34 event beds include both the analysis of the sandstone layer and that of the co-genetic mudstone cap.

Mineralogical composition of the mudstones was carried out through X-ray Powder Diffractometry (XRPD) on untreated samples (Nat), and after the standard treatments for the identification of the clay minerals: ethylene-glycol saturation (Gly) for the identification of the swelling clay minerals and heating at 550ºC. The analysis was carried out using PW1800/10 Philips X-ray Diffractometer and

X'Pert High Score - v. 4.6a software (PANalytical B.V.), Cu Kα, graphite monocromator, 45Kv - 35mA, 2° - 65° 2θ, speed 0.02° 2θ/sec. The results from the XRPD analyses have been compared with those in ICDD (International Centre for Diffraction Data) database and with our reference standards, to obtain a qualitative mineralogical composition. Semi-quantitative analysis was performed according to the approach of Biscaye (1965) and Moore and Reynolds (1989). Recognised species included quartz, k-feldspar, plagioclase, carbonates (calcite and dolomite) and phyllosilicates (chlorite, serpentine, muscovite-illite and smectite). The full dataset is presented in the supplementary material.

4. Results

4.1 Thickness data

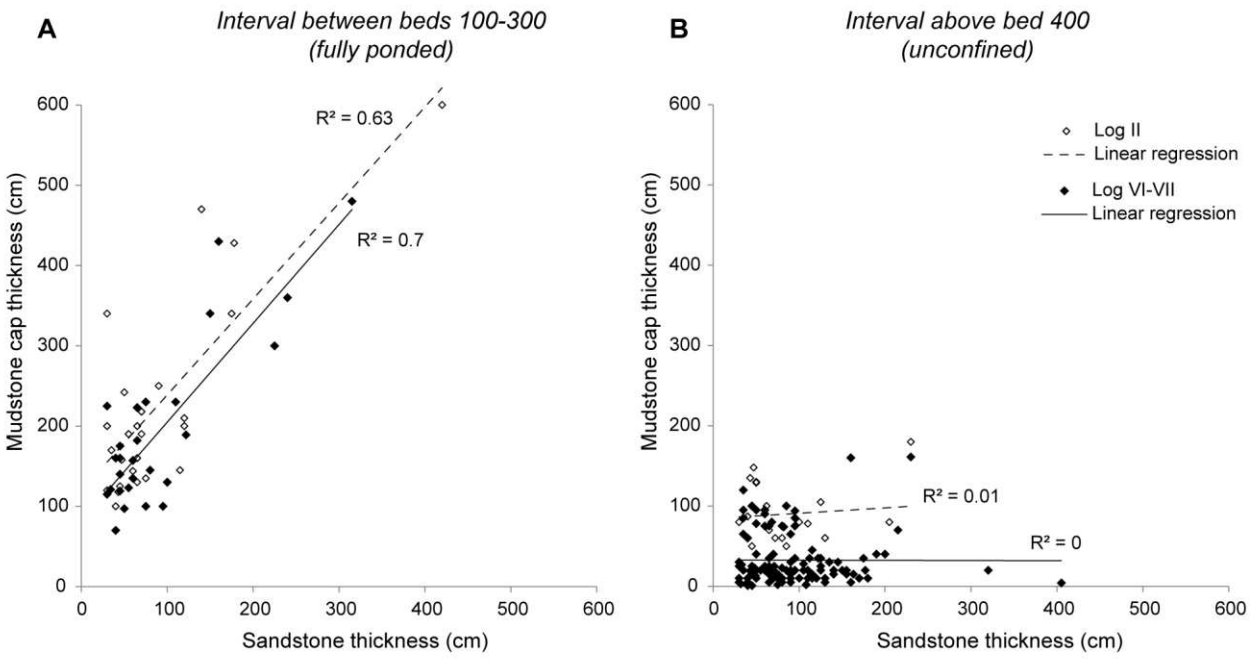

Figure 5. Sandstone thickness vs associated mudstone cap thickness for sandstone beds 0.3-6 m thick (turbidites only). A) Fully ponded interval (between beds 100 and 300) and B) unconfined interval (above bed 400). For logs and localities, see Fig. 2C-D.

For the purpose of comparing bed thicknesses, two intervals were selected: a c. 400 m thick interval between bed 100 and 300 (the lower part of the ponded interval recognised by Marini et al., 2016A) and a c. 200 m thick interval above bed 400 (part of the transitional and unconfined units of Marini et

al., 2016A; see also Fig. 2D). The choice of restricting the bed thickness analysis to the lower part of the ponded interval was based on the consideration mentioned above that ponding depends on the size of the event and that in a sequence evolving from fully ponded to unconfined an extensive transitional interval (characterised by mud from smaller and smaller events being able to spill) should be expected.

For medium to thick turbidite beds (sandstone thicker than 29 cm) the investigated ponded interval of the Castagnola turbidite system is characterised by a positive correlation between the sandstone thickness and that of its co-generic mudstone cap (Fig. 5A; see also Marini et al., 2016A). This is in contrast with the absence of any relationship in the upper unconfined interval (Fig. 5B). The existence of a direct relationship between the thickness of the sandstones and that of their associated mudstone layers in the ponded interval provides evidence that the mudstones were deposited as part of the same event or chain of events (mudstone caps *sensu stricto*; T_e of Bouma, 1962; Haughton, 1994). The relationship can be explained as an effect of the local confining topography on the geometry of both the sandstone layers and of that of the associated mudstone layers. The trapping of the flows against the confining slopes of an enclosed basin results in more tabular geometries of deposit (e.g., Marini et al., 2015; Liu et al., 2018; Tőkés and Patacci, 2018) and in the deposition of the mud in the same area of the sand (see definition of ponding in the introduction), directly translating the sand to mud ratio of the parent flows into thickness ratios. This is because the lenticular convex-upward depositional geometry characteristic of a sandy layer deposited by an unconfined flow event (e.g., Baas et al., 2004) cannot be developed and bypass of the mud toward deeper locations further down-dip is prevented.

The positive correlation shown for turbidites is also observed for hybrid event beds, although they usually have mudstone caps only one quarter to one half as thick as those of turbidites of similar sandstone thickness. On a sandstone vs mudstone thickness plot, turbidites and hybrid event beds therefore plot into distinct spaces, which are divided by the 1:1 sand-to-mud ratio line (Fig. 6).

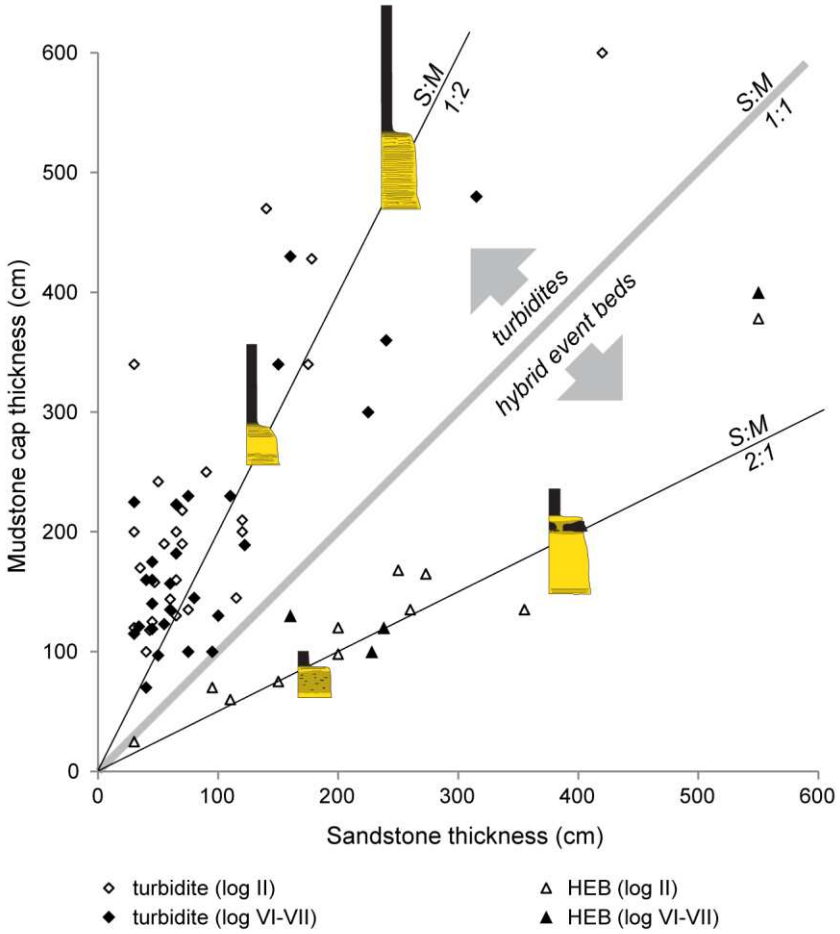

Figure 6. Sandstone thickness vs associated mudstone cap thickness for sandstone beds 0.3-6 m thick (turbidites and hybrid event beds). Data from the fully ponded interval (between beds 100 and 300), roughly 400 m thick. Number of bed measurements plotted: 68 (29 bed measurements have been discarded due to poor exposure). For log localities, see Fig. 2C-D. Note that the data for turbidites are the same as in Fig. 5A.

It should be noted that the “sandstone” part of hybrid event beds includes significantly more clay than that of turbidites because of the presence of clay matrix and mudstone clasts in the H3 division (Porten et al 2016; Fonnesu et al., 2018), raising the possibility that the different bed types have similar proportions of sand and mud, albeit differently distributed. This hypothesis was tested for a selected number of beds by conceptually removing the clay from each “sandstone” interval (i.e. thinning it) and adding it to the associated mudstone cap (thickening it). The test was based on the detailed logs of the hybrid beds and supported by Southern et al., 2015 log panels to estimate the average thickness of the H3 division. A range of values for the H3 division clay content were tested, from 25% to 75%, as the actual value could not be measured quantitatively. The results indicate that even choosing the

more conservative value of 75% clay for H3 divisions, the correction can only account for a proportion of the relatively greater thickness of the turbidite mudstone caps; this is also evident by comparing the examples of Fig. 3. However, quantitative characterisation of the average clay content within the H3 division of hybrid event beds along a long transect remains an area of future research, needed to better understanding the partitioning of clay in this type of deposits.

In summary, the datasets of Figs. 5 and 6 suggest that the sandstone to mudstone cap ratio is linked to the event bed type and therefore must provide some meaningful insight into the emplacement mechanism of turbidites vs hybrid event beds. In conjunction with the bed thickness analysis and in order to provide an additional prospective on the origin and transport history of the sand and mud in each flow event, a petrographic analysis of sandstones and a mineralogic analysis of mudstones were undertaken. Their results are especially insightful because in the Castagnola system beds with striking contrasting provenance and composition are known to be interbedded (Cibin et al., 2003).

4.2 Sandstone provenance data

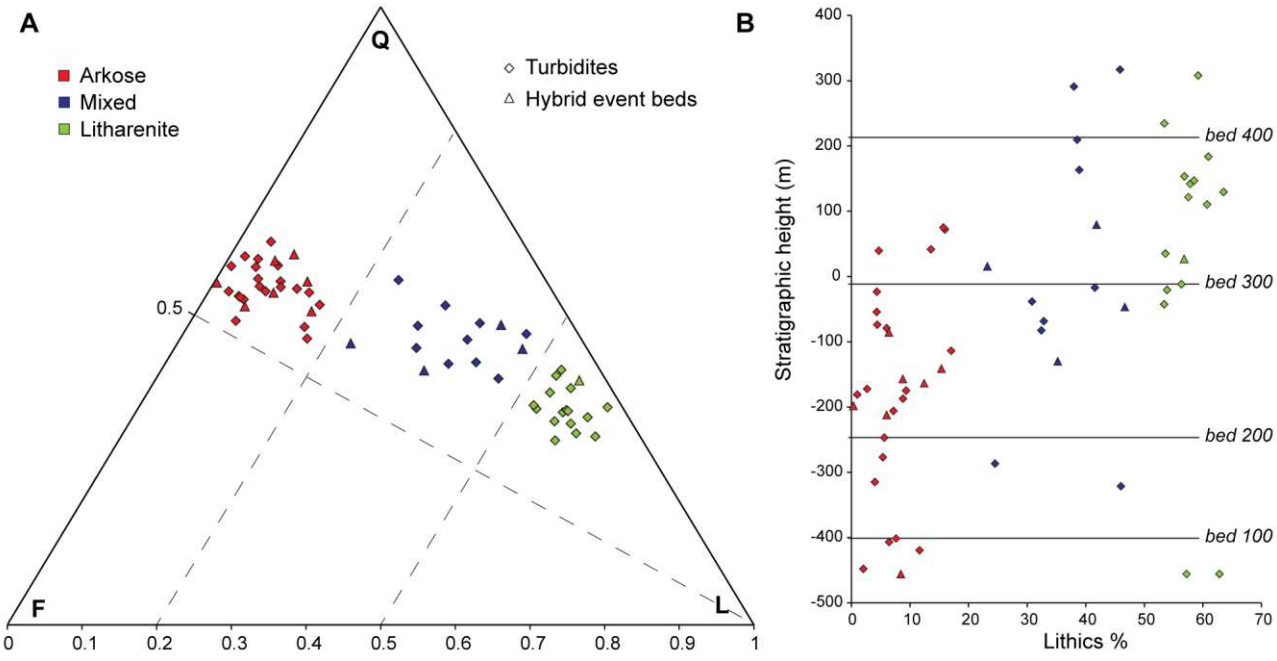

Figure 7. Sandstone petrography (for beds >29 cm thick) plotted on a standard QFL diagram (A) and as lithics percentage vs stratigraphic height (B) of the bed base (top of bed 300 is used as datum). Data shown for all sampled beds (59 out of 113 beds >29 cm thick in the interval up to bed 433).

A QFL triangular plot of the Castagnola sandstones petrography shows a wide range of petrographic signatures (Fig. 7A). Two different sandstones types can be clearly recognised: an arkosic one (clustering at around 10% lithics) and a litharenitic one (around 60% lithics), with some data points showing a more mixed composition. Overall, there is an upward stratigraphic evolution from most beds being arkosic to most beds being litharenitic (Fig. 7B). However, some litharenites can be found in the lower part of the section as well. The two petrographic types can be related to the different terrains inferred to have provided the source for the sediment (Cibin et al., 2003). Based on outcrop relationships in the south of the TPB, the arkosic sands are interpreted to be sourced by continental basement units with limited Permian cover (Savona Massif?; Fig. 2A-B), while the litharenitic sands record a provenance from Voltri Group high-pressure Alpine metamorphic units (Fig. 2A) largely comprising serpentinite oceanic units (e.g. Barbieri et al., 2003; Carrapa et al., 2004).

4.3 Mudstone composition data

In order to interpret the mudstone composition data in the context of the two sandstone types described above, the serpentine mineral group was chosen as the best index mineral to highlight the association (or lack thereof) of a mudstone with a lithic source. This group of minerals is not diagenetic at the burial conditions of the Castagnola (Di Giulio et al., 2002) and is therefore associated with the weathering and erosion of the meta-ophiolite terrain that is inferred to have been the source for the litharenites (Voltri Group; Fig 2A; see also Cibin et al. 2003). Additionally, it is expected to be virtually absent in mudstones resulting from the weathering and erosion of the continental basement arkosic terrain that sourced the arkosic sands (see for instance Ibbeken and Schleyer, 1991 for a modern analogue). Because of the likely similar diagenetic conditions experienced by all the samples, no correction was applied to the measured proportion of serpentine group minerals.

The measured values of serpentine proportions are clustered at around 10-16% and hence they show that mudstone caps have a more mixed compositional signature than the sandstones (compare histograms of Fig. 8A and B). Although some direct relationship between sandstone and mudstone composition can be observed (mudstone caps associated to arkosic sandstones have generally lower

serpentine values; Fig. 8B), it is very weak, as also illustrated by the scatter plot of Fig. 9A. The lack of a strong relationship is true for both turbidites and hybrid event beds.

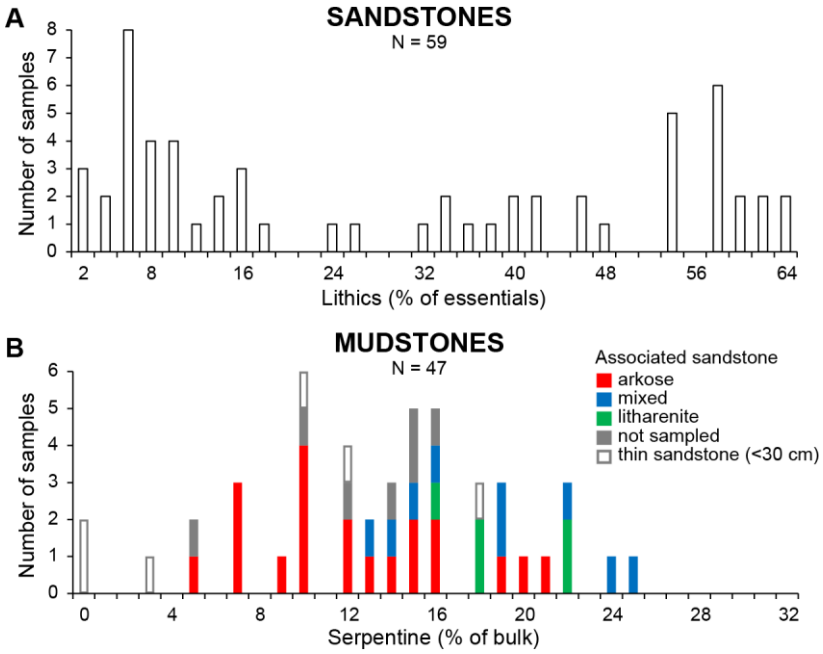

Figure 8. Histograms showing A) proportion of lithics in sandstones (% of essential sandstone grains) and B) proportion of serpentine minerals in mudstones (% of bulk mudstone). Bars for the mudstones are colour coded based on the composition of the underlying co-genetic sandstone. Labels on the x-axis indicate the upper limit of each bin. Six measurements from mudstone caps of thin beds (<30 cm) have been included in part B to document the full variability of mudstone composition present in the basin, although these beds are not considered when computing sandstone to mudstone thickness ratios.

4.4 Mixing model

The petrographic analysis illustrates that the Castagnola depocentre was filled by sediment sourced from two principal terrains. Each terrain in isolation must have produced an end-member composition of sands and muds: one is arkosic (sand composed of dominantly Q-F grains with no fine-grained lithics and muds with no serpentine) and the other litharenitic (sand composed of dominantly L-Q grains with very limited feldspar grains and muds rich in serpentine). The sandstone samples show that most individual gravity flow events transported sand primarily sourced from one terrain. Less than a quarter of the events transported mixed sands (Fig. 7), possibly generated either by direct discharge

from rivers whose catchment included both terrains or by contemporaneous discharge and/or remobilisation of sediment from different river catchments.

By using the serpentine group minerals as an indicator of mud generated by the lithic terrain, the mudstone XRD analysis shows that the composition of the mudstone caps is more mixed than that of their co-genetic turbidite sandstones (Fig. 8). In order to understand what processes might have caused this different degree of mixing, a mixing model can be devised. In the simplest case, it is possible to assume that if an event carried sediment composed in equal proportions of lithic and arkosic sand, the mud would be mixed in equal proportions as well. In this scenario, plotting the percentage of lithics in the sand against the percentage of serpentine in the mud should result in a linear correlation (Fig. 9A). Each end-point of the mixing line should correspond to one of the end-members. A slight variation of this model can be envisaged if the two sources are associated with different sand-to-mud ratios (e.g. the lithic source might have a primary sand-to-mud ratio a quarter that of the arkosic source; $m_L = 4m_A$), resulting in curved mixing lines (Fig. 9B). It should be noted that these ratios could reflect true sand-to-mud ratios of the sediment delivered by rivers or could result from the two sources having different mechanisms or intensity of sediment partitioning on the shelf.

In order to plot the mixing lines on Fig. 9B, the composition of the two ideal end members needs to be estimated. The arkosic terrain in isolation can be considered to generate sand containing no lithics and mud containing no serpentine. Although none of the sampled bed has this composition, there are sandstone beds with almost no lithics (2 samples <2%; Fig. 8A). In addition, two out of six samples of mudstones associated with thin beds have no serpentine (Fig. 8B), confirming that this type of mud existed in the system.

By contrast, the proportions of lithics (in the sand) and serpentine (in the mud) generated by the lithic source in isolation are less easy to estimate. However, the choice of the ideal lithic end-member (sand and mud) has a smaller overall impact on the mixing model results than the choice of the sand-to-mud ratio of the sources. The sand can be assumed to comprise 64% lithics, which represent the highest amount in any of the sampled sandstones. The proportion of serpentine in the muds

associated with the 'pure' lithic source also needs to be estimated. The lower limit of its possible range of values could be constrained by the highest measured value of serpentine, defining a lower bound of 25%. However, this sample has an associated sandstone lithics percentage of only 47%, suggesting that the proportion of serpentine in the mud ideally associated with the end-member sandstone (64% lithics) should be greater. A value of 30% was chosen based on the best linear fit (intersecting the origin; Fig. 9A).

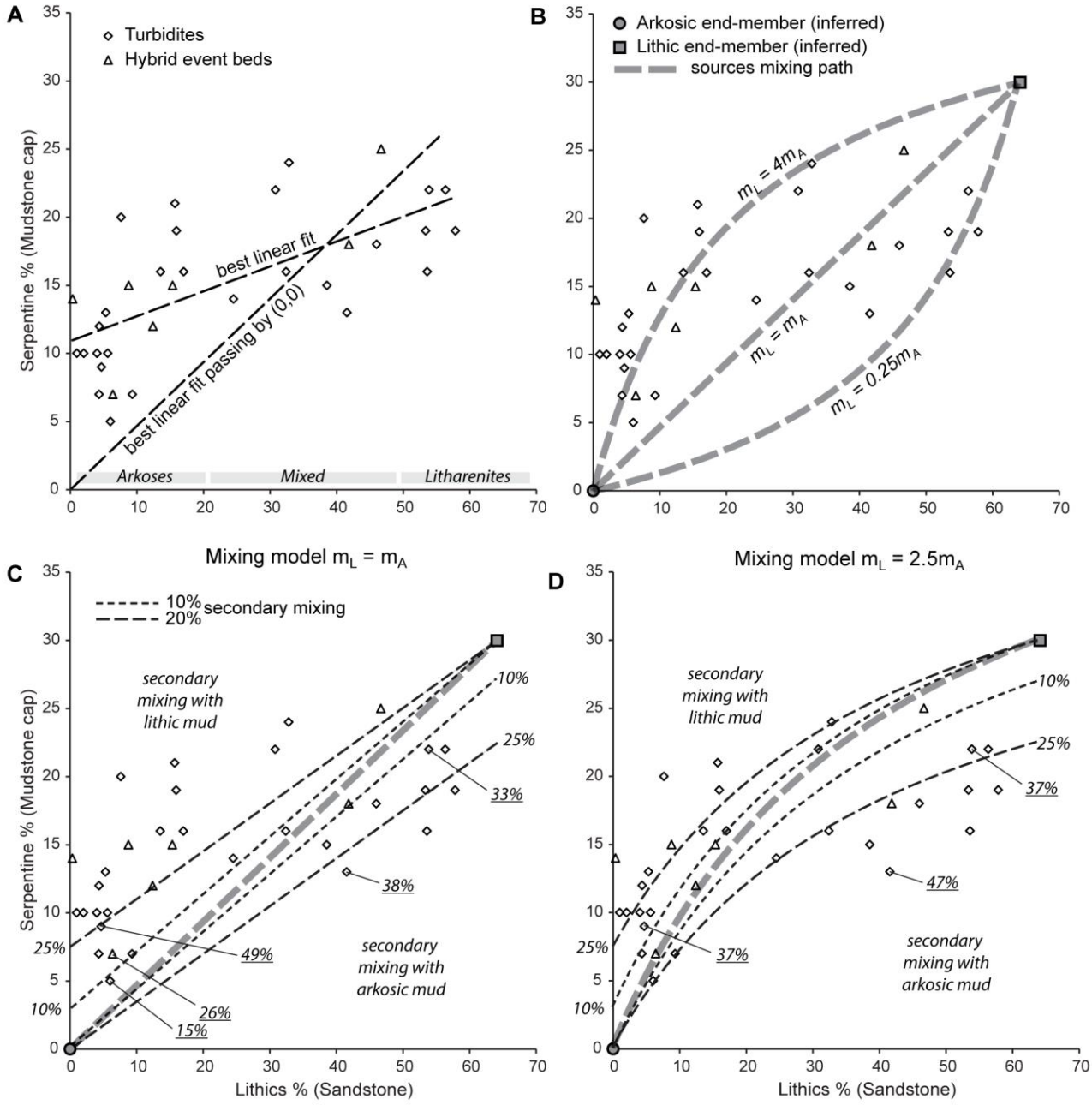

Figure 9. Composition of sandstone (expressed as percentage of lithic grains) vs composition of its mudstone cap (expressed as percentage of serpentine minerals). Same dataset as Figs. 7 and 8, but

only 34 beds with both sandstone and mudstone analyses are plotted. A) Best linear fit and best linear fit intersecting the origin. B) Mixing paths for three different mixing models with sources (end-members) with different sand-to-mud ratios (mL and mA represent the amount of mud associated with the lithic and the arkosic source, respectively). The mixing paths represent all the compositions that can be obtained if the two end members are mixed in various proportions, assuming both sand and mud are mixed. Points plotting away from a mixing line imply a more complex mixing story. C-D) Mixing models for two scenarios (C: lithic and the arkosic source have the same sand-to-mud ratio; D: lithic source is associated with 2.5 times the mud of the arkosic source). Points plotting above the mixing line (thick dashed grey line) have been mixed with lithic mud, the ones below with akosic mud. Black dashed lines indicate 10% and 25% minimum amount of secondary mixing (assumes mixing with opposite end-member mud). Underlined percentages refer to the degree of secondary mixing that must have occurred if the mixed mud was sourced directly from the substrate of the sample bed (rather than being an arkosic or lithic mud end-member).

The distribution of the data points of Fig. 9B indicates that regardless of the mixing model chosen or of the position of the lithic source end-member, a significant portion of the data plot consistently away from any individual mixing line. Hence, it appears that a simple mixing model where two sources of sand and mud mix in variable proportions cannot reproduce the compositional range of the data. A more sophisticated model can be devised, including two phases of mixing, a first one with sand and mud mixed in their original relative proportions and a second one with only the mud component being mixed. Mixing of the first type should be expected in the case of direct discharge from rivers whose catchment included both terrains or in the case of contemporaneous discharge or remobilisation of sediment from different river catchments, and will be called 'primary mixing'. The amount of 'primary mixing' is likely more revealing of the local geographic configuration than of sedimentary processes. The second phase of mixing or 'secondary mixing' is characterised by the mixing of the mud component only, and indicates the ability of sedimentary processes to mix the muds, but not the sands. The amount of secondary mixing is therefore related to the importance of such processes. Possible mechanisms of secondary mixing are discussed in detail below (section 4.5).

Mixing models for two scenarios (characterised by different sand-to-mud ratios of the sources) are presented in Fig. 9C-D. In addition to the 'primary' mixing lines (thick dashed grey lines), additional thin dashed black lines indicate contours for 10% and 25% of secondary mixing (i.e. 10% or 25% of the mud has been added during secondary mixing; 10% and 25% are not special amounts and they

are simply shown for reference). These lines are calculated by assuming that the observed shift away from the mixing line is due to secondary mixing with an opposite end-member mud (i.e. for a point falling below the mixing line, it is assumed that the secondary mixing involved pure lithic mud containing 30% serpentine). This assumption means that the dashed black lines of Fig. 9C-D represent minimum estimates of secondary mixing as mixing with any other type of mud will result in higher values. In the hypothesis that the 'secondary mixing' is linked to erosion of the substrate in the basin (see discussion below; section 4.5), for those beds for which substrate composition is available it is possible to calculate a better estimate of how much mud from the substrate was mixed with the end member mud associated with the sand lithotype. The results of this calculation are shown as underlined percentages in Fig. 9C-D.

In conclusion, although the deterministic calculation of the percentage of mud which was added by 'secondary mixing' processes is not possible with the available data, a range of plausible scenarios suggest a majority of beds experienced significant 'secondary mixing' and that on average at least 1/4 to 1/3 of the mud deposited in the basin was added after primary source mixing.

4.5 Process interpretation of secondary mixing

The data summarised in Fig. 9 show that a secondary process or processes resulted in the mudstones deposited in the basin being more mixed than their co-genetic sandstones. A number of erosional features at the base of turbidite beds are seen in the basin, such as cm-high steps at the base of beds (cf. 'delamination' of Fonnesu et al., 2016). This suggests that the 'secondary mixing' could be associated with mud acquisition through substrate erosion along the submarine routing system, in the basin or on the confining slopes. Alternatively, the mixing could have occurred while the sediment was stored on the shelf or on a delta front due to selective mixing of the mud (Macquaker et al., 2010).

The first interpretation is favoured because of the outcrop evidence showing that flows were erosive even in the outcropping distal part of the system (Southern et al., 2015); more significant erosion may have occurred in more proximal parts of the flow pathways. Although it cannot be discounted, shelf

re-working is also deemed less likely because of the inferred steep gradients and narrow shelf characterising the local palaeogeography (Rossi and Craig, 2016).

5. Discussion

5.1 Thickness versus volume

An assumption is made that most of the mudstone caps and the sandstones considered in the analysis (thickness > 29 cm) are fully ponded (i.e. both the sandy and muddy parts of the flow were interacting with and contained by a bathymetric low) and hence have a highly tabular geometry (*sensu* Tőkés and Patacci, 2018). It follows that their thickness represents a good proxy for the volume of sand and mud transported to the distal part of the system. The ponding interpretation is supported by facies and bed thickness statistics (Marini et al., 2016A; 2016B) and the tabularity by the high bed continuity and very low thinning rates (0.15-0.05 m/Km for beds 0.3-1.5 m thick) at the >2 Km scale (see also Southern et al., 2015; Tőkés and Patacci, 2018). However, this assumption could be invalid if the beds considered are not highly tabular outside of the observation window and if the different bed types have different depositional geometries (cf. Amy et al., 2005). This is difficult to assess in the Castagnola system, as the most distal part of the basin is not preserved due to recent uplift and erosion (see section 5.2 below on how to address this uncertainty). Additionally, it should be noted that a minority of the beds, in particular HEBs, show significant thickness changes (e.g., beds 203 and 212; Southern et al., 2015). These beds have not been included in the main analysis. Finally, HEBs are usually more common in lateral/distal fringes of lobes (Haughton et al., 2009; Kane et al., 2017; Spychala et al., 2017), although this is not always the case (e.g., Mueller et al., 2017). However, this is not expected to cause a significant bias in the thickness dataset (between beds 100 and 300) as there is no consistent evolution from a less hybrid prone to a more hybrid prone interval or vice versa, which could be explained as a progradation or retrogradation trend in a distally-unconfined system (possibly associated with different mudcap thicknesses). Therefore, despite caveats, the assumption that sandstone and mudstone thicknesses represent a good proxy for the volume of sand and mud transported to the distal part of the system appears reasonable.

5.2 Observations from other turbidite systems

In order to overcome some of the limitations related to the Castagnola dataset (namely the limited preserved portion of the turbidite system), other systems can be compared to test the observed relationship between sandstone and mudstone thickness in turbidites and hybrid event beds. Some authors have published illustrations of bed types that include thicker mudstone caps for turbidites compared to HEBs (e.g., Fig. 14 of Hovikoski et al., 2016), but without an accompanying discussion. In order to confirm that the observed differences in sand-to-mud ratios are not only due to the different geometry of the beds but represent a real difference in the sand to mud volumetric ratio, a confined system with very long-distance correlations should be considered. The Marnoso-arenacea Formation of central Italy (Tinterri and Tagliaferri, 2015) provides a number of suitable published datasets from the confined Langhian to Serravallian succession, to test whether sand to mud ratios of turbidites and hybrid events beds are systematically different, thanks to very long-distance correlations (including the very distal part of the system) and to high-resolution data on sandstone and mudstone cap thicknesses.

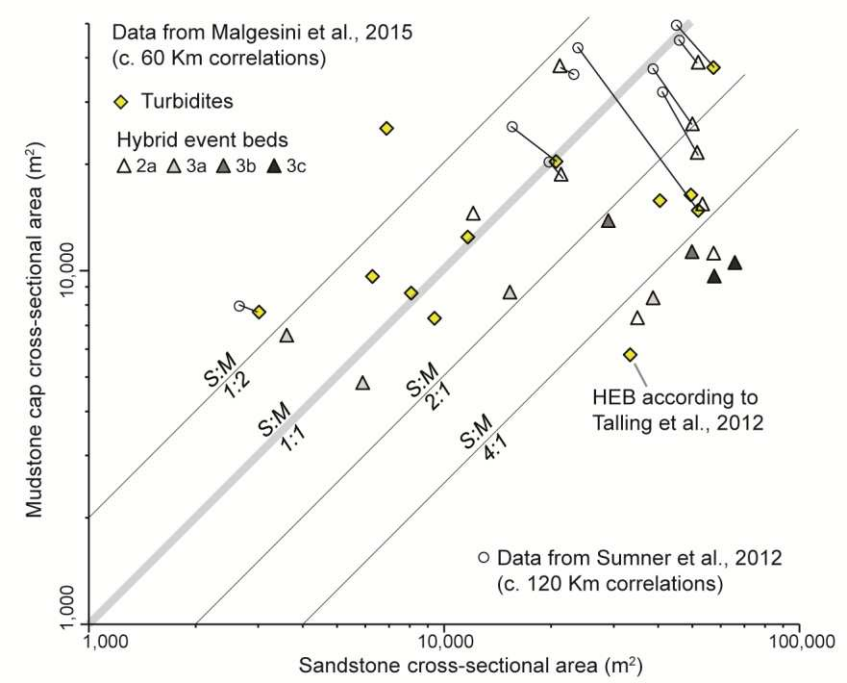

Figure 10. Cross sectional area along depositional dip for sandstones and their associated mudstones for a number of beds just below or above the Contessa marker bed (Marnoso-arenacea Formation). Primary data comes from 60 km long cross-sections by Malgesini et al., 2015. Additional data for a

selection of the same beds is calculated from 120 km long cross-sections by Sumner et al., 2012 (shown by circles; black lines link the two datasets). Note that, to facilitate comparison, the Sumner et al. dataset was calculated on the entire 120 Km long cross-section and then adjusted so that total area (sandstone + mudstone) would be equal to that of the corresponding bed in the Malgesini et al. dataset.

Figure 10 presents cross-sectional areas along depositional dip from 29 sandstone beds (ranging from 20 to 170 cm thick) and their associated mudstone caps (data from Malgesini et al., 2015 and Sumner et al., 2012). Of those, 11 are turbidites and the rest are hybrid event beds that include a muddy chaotic division (classification based on facies tracts by Malgesini et al., 2015). The only two beds with a sand-to-mud ratio less than 1:2 are turbidites. Of the six beds with a sand-to-mud ratio greater than 4:1, five are HEBs and the sixth is classified as a turbidite by Malgesini et al. (2015), but as a HEB by Talling et al. (2012). Overall, 3 turbidites and 12 HEBs have more sand than mud, while 8 turbidites and 3 HEBs have more mud than sand. Although the results are not as clear-cut as those from the Castagnola, it appears that generally turbidites are associated with larger mudstone caps than HEBs, shown in this case using data calculated along a very long transect that – for the Sumner dataset in particular – reaches into the very distal part of the basin, although not necessarily the down-dip termination of each event bed. The Marnoso-arenacea sand to mud ratios therefore incorporate the difference in geometry of the different bed types that have been recognised in this system (Amy et al., 2005); as noted above, in the Castagnola dataset such differences in bed geometry are very rarely observed in the preserved basin, but could have existed elsewhere.

Additionally, the Marnoso-arenacea dataset allows a more reliable estimation of the full clay volume for individual flow deposits than those calculated from the Castagnola. In most of the turbidite beds from the Marnoso-arenacea system presented in Fig. 10 compacted mud accounts for more than 50% of the total deposit volume (decompaction would increase this value). The calculation considers the last 120 km or so of a larger depositional system and it is not known much about what happens up-dip (due to difficulty in correlation and lack of outcrop). However, this is not an issue for understanding the behaviour of the flow in the basin, because what was deposited up-dip was not in the flow any longer along the observed transect. Similarly, even in the data-rich Marnoso-Arenacea system the

calculated mud percentage might increase given a better characterisation of the muddy deposits in the most distal part of the basin. Finally, the Marnoso-arenacea is known to include beds with different sources (e.g., Gandolfi et al., 1983 among others). Thus, it might be possible to compare sandstone petrography and mudstone compositions to refine and better interpret the data in Fig. 10 in a similar fashion to the analysis that has been presented for the Castagnola system.

5.3 Mud volume, flow behaviour and depositional processes

The presented data and the considerations highlighted in the previous sections suggests that: i) flows that deposited turbidites are associated with larger amounts of clay (often >50% by volume) than those depositing HEBs, and ii) a significant proportion of the total clay in both flow types is likely acquired en-route. It follows that the flows associated with larger amount of clay eroded larger volumes of substrate and that they preferentially deposited clean turbidites. Sandier flows eroded smaller volumes of substrate and were more likely to deposit hybrid event beds. It should be noted that although these conclusions are derived from the data acquired from the Castagnola system and reinforced by the analysis of data from the Marnoso-arenacea formation - both ponded systems - there is reason to expect that they might be valid more generally and also for unconfined turbidite systems.

To investigate the differences in flow evolution that led to the two types of deposit, it is first necessary to consider where the mud might have been held in the flow. If all the mud in the deposit was transported immediately alongside the sand, a mixed deposit (possibly a ‘muddy debrite’) might be expected. As this is not what is observed, it follows that the flows that deposited turbidites must have been relatively efficient at fractionating their mud into the upper and/or rear parts of the flow, resulting in the development of a thick, low-density mud cloud (cf. flows monitored in the Congo Fan; Azpiroz-Zabala et al., 2017). By contrast, flows that deposited hybrid event beds must have been less effective at fractionating mud, as their deposits include a division with the character of a muddy debrite. Additionally, the observations from the Castagnola system suggest that both types of flow were erosive, but that the muddier flows were more erosive; the erosive capacity of muddy flows has been

established elsewhere (e.g., the 1929 Grand Banks turbidity current was initially muddy, eroding all its sand en-route; Piper et al., 1999). It is worth noting that erosion of muddy substrate and mud segregation in the flow work to augment vs diminish the amount of dispersed clay in the basal layer of the flow, respectively.

The balance between the erosion of muddy substrate and segregation of mud into higher zones of the flow may control the likelihood of occurrence of a rheological change and therefore control the deposition of a turbidite or of a hybrid event bed. In other words, flows that remain as turbidity currents must erode enough mud to remain turbulent or to become turbulence enhanced (*sensu* Baas et al., 2009), but not enough to become transitionally turbulent or laminar, with the balance moderated by mud segregation away from the basal flow. The balance must be different for flows that evolve to become hybrid in character. The key question is what controls if the flow is muddy and erosive, but able to fractionate the clay, or sandier and less erosional, but also less able to fractionate the clay. Arguably the amount of clay in the original flow is a likely primary control; the data permit a tentative suggestion that the parent flows of the turbidites originally had more mud even before en-route mud acquisition through erosion. This is shown by the weak correlation between the composition of the sandstone and that of the associated mudstones (Fig. 8B); not all the mud is acquired en-route.

The type of substrate could also play a role. For example, a softer substrate could favour mud entrainment and fractionation and result in the deposition of a turbidite (cf. Baas et al., 2016). Although in principle this mechanism could work, it appears unlikely to be significant. Fluid mud is rarely in a state of equilibrium (i.e. a state in which the thickness remains constant for long periods) and it is usually compacting and forming a hard bed (a process that may take 10-20 years; see table 8.1 in Mehta, (2014), although thicker layers might take longer to consolidate). In addition, phenomena like liquefaction of mud usually only occur up to 25 days from deposition (Mehta, 2014), so are unlikely to happen under a turbidity current unless the frequency of large events is very high (cf. Gutierrez-Pastor et al., 2009; Allin et al., 2016).

Finally, the flow speed, thickness and concentration (yielding mass flux) combined with its duration (to give total sediment volume) could also play a role. The importance of this control is suggested by the different sedimentary structures preserved in the sandy part of the beds. The almost complete lack of sedimentary structures in HEB H1 division points toward short duration-high flux flow (i.e., with associated high aggradation rates), while the abundance of traction features in turbidites is suggestive of long duration-low flux flow (Lowe, 1988; Mulder and Alexander, 2001). Interestingly, long duration turbidity currents might not require mud erosion and fractionation rates higher than those of hybrid flows; by occurring over a much longer time, low erosion rates could account for the greater cumulative erosion. It is inferred that what controls the likelihood of turbidity current to hybrid flow transition is the ratio between the rates of mud erosion vs fractionation; the fractionation rate must equal or exceed the erosion rate for flows to remain as turbidity currents.

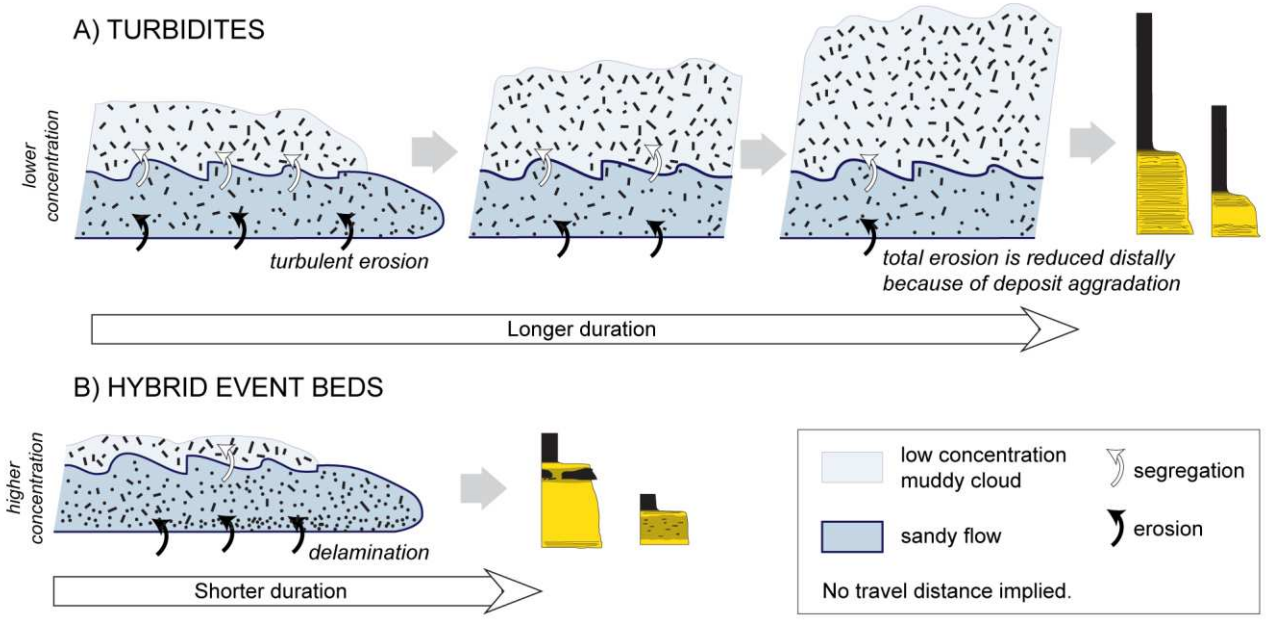

Figure 11. Inferred flow types and their evolution accounting for the deposition of turbidites (A) and hybrid event beds (B) in the ponded interval of the Castagnola system. Low density, long duration, erosive, muddy flows depositing turbidites and higher concentration-shorter duration, less erosive and sandier flows depositing hybrid event beds. Note that the figure does not attempt to compare instantaneous erosion rate, nor the thickness of the sandy part of the flows between the two flow types (shown as equal).

In summary, it appears that two types of flows alternated in the Castagnola system: 1) relatively low density, long duration, muddy flows depositing turbidites and 2) higher concentration-shorter duration, sandier flows depositing HEBs (Fig. 11). As noted above, the first type may result in larger cumulative erosion. The two classes of flow types may link to different types of trigger (e.g., Talling, 2014), such that long duration muddy flows could initiate from hyperpycnal events and shorter duration sandier flows to delta failures due to over steepening and/or seismic shocks, although the presented data do not allow confirmation of this idea.

The conclusions from this study do not fit with the concept that hybrid beds are typically more enriched in mud than turbidites; the concept is still valid if considering only the "sandstone part" of the event, but – it is argued here – not when considering the entire event, including its mudstone cap and its distal mudstone. Additionally, the focus on the erosional character of hybrid bed parent flows, e.g., due to out-of-grade slopes (Haughton et al., 2009) or high drop height (Pierce et al., 2018) should be balanced by the recognition of their more limited total erosional capacity when compared to turbidity currents. These conclusions need not necessarily be specific to ponded systems; more research on the distal mudstone deposits of unconfined systems is required to confirm their broader applicability. Finally, although this paper has not differentiated types of hybrid event beds (HEBs), there is growing recognition that different families of hybrid flow may occur, producing HEBs of different character (e.g., Talling, 2013, Fonnesu et al., 2018; Pierce et al., 2018). Further research is required to explore whether and how the conclusions of this paper apply to the full range of hybrid event bed types.

6. Conclusions

- Ratios of sandstone to mudstone cap thickness tie systematically to turbidite vs HEB bed type in the Castagnola sheet-like ponded succession. Hybrid event beds have thinner mudstone caps than turbidites, suggesting that they are associated to smaller mudstone volumes in the basin. This is also supported by long-correlation bed data from the Marnoso-arenacea formation. The implication is that the parental hybrid flows carry less total mud in the basin than turbidity currents.

- Mudstone cap analysis can provide invaluable insight into erosional and depositional processes of their depositing currents (whether turbidity currents or hybrid flows); in the Castagnola system muddier flows of likely longer duration were cumulatively more erosive, but deposited clean sandstones, whereas sandier flows of likely shorter duration were less erosive, but deposited hybrid event beds.
- Mud entertainment rate vs fractionation rate is a key control on clay concentration in the basal layer of the flow and therefore on the likelihood of rheological transformation from turbidity current to hybrid flow.

Acknowledgements

Many thanks to Vanessa Fontana, Christian Boatti and Claudia Desogus (students at the Universities of Pavia and Milan) for carrying out some of the sandstones point counts. Reviewers Arnau Obradors-Latre, Yvonne Spychala and Colm Pierce and associate editor Anna Pontén are also thanked for providing valuable comments that helped improve the final version of the manuscript. The Turbidites Research Group sponsors (AkerBP, BP, ConocoPhillips, Equinor, Eni, Hess, Murphy, OMV and Shell) are thanked for their financial support.

References

Al Ja'Aidi, O.S., McCaffrey, W.D. and Kneller, B.C. (2004) Factors influencing the deposit geometry of experimental turbidity currents: implications for sand-body architecture in confined basins. In: Confined Turbidite Systems (Eds. S.A. Lomas and P. Joseph), Geological Society of London Special Publication, 222, 45-58.

Allin, J.R., Hunt, J.E., Tailing, P.J., Clare, M.A., Pope, E. and Masson, D. G. (2016) Different frequencies and triggers of canyon filling and flushing events in Nazare Canyon, offshore Portugal. Marine Geology, 371, 89-105.

Amy, L.A., Talling, P.J., Peakall, J., Wynn, R.B. and Thynne, R.G.A. (2005) Bed geometry used to test recognition criteria of turbidites and (sandy) debrites. Sedimentary Geology, 179(1-2), 163-174.

Andreoni, G., Galbiati, B., Maccabruni, A. and Vercesi, P.L. (1981) Stratigrafia e paleogeografia dei depositi Oligocenici Sup.-Miocenici Inf. nell'estremità orientale del Bacino Ligure-Piemontese [Translated Title: Stratigraphy and paleogeography of the Upper Oligocene-Lower Miocene deposits of the western extremity of the Ligure-Piemontese Basin]. Rivista Italiana di Paleontologia e Stratigrafia, 87(2), 245-282.

Angus, K., Arnott, R.W.C and Terlaky, V. (2019) Lateral and vertical juxtaposition of matrix-rich and matrix-poor lithologies caused by particle settling in mixed mud–sand deep-marine sediment suspensions. Sedimentology, 66(3), 940-962.

Azpiroz-Zabala, M., Cartigny, M.J.B., Talling, P.J., Parsons, D.R., Sumner, E.J., Clare, M.A., Simmons, S.M., Cooper, C. and Pope, E.L. (2017) Newly recognized turbidity current structure can explain prolonged flushing of submarine canyons. Science Advances 3(10), 12.

Baas, J.H., van Kesteren, W. and Postma, G. (2004) Deposits of depletive high-density turbidity currents; a flume analogue of bed geometry, structure and texture. Sedimentology, 51(5), 1053-1088.

Baas, J.H., Best, J.L., Peakall, J. and Wang, M. (2009) A Phase Diagram for Turbulent, Transitional, and Laminar Clay Suspension Flows. Journal of Sedimentary Research, 79(3-4), 162-183.

Baas, J.H., Manica, R., Puhl, E. and Borges, A.L.D. (2016) Thresholds of intrabed flow and other interactions of turbidity currents with soft muddy substrates. Sedimentology, 63(7), 2002-2036.

Baker, M.L., Baas, J.H., Malarkey, J., Silva Jacinto, R., Craig, M.J., Kane, I.A. and Barker, S. (2017) The Effect of Clay Type On the Properties of Cohesive Sediment Gravity Flows and Their Deposits. Journal of Sedimentary Research, 87(11), 1176-1195.

Barbieri, C., Carrapa, B., Di Giulio, A., Wijbrans, J., Murrel, G. (2003) Provenance of Oligocene synorogenic sediments of the Ligurian Alps (NW Italy): inferences on belt age and cooling history. International Journal of Earth Sciences, 92, 758-778.

Baruffini, L., Cavalli, C. and Papani, L. (1994) Detailed stratal correlation and stacking patterns of the Gremiasco and lower Castagnola turbidite systems, Tertiary Piedmont Basin, northwestern Italy. In: "Submarine Fans and Turbidite Systems: Sequence Stratigraphy, Reservoir Architecture and Production Characteristics, Gulf of Mexico and International" (Eds. P. Weimer, A.H. Bouma and B.F. Perkins), GCSSEPM Foundation 15th Annual Research Conference, 9-21.

Bell, D., Kane, I.A., Pontén, A.S.M., Flint, S.S., Hodgson, D.M. and Barrett, B.J. (2018) Spatial variability in depositional reservoir quality of deep-water channel-fill and lobe deposits. Marine and Petroleum Geology, 98, 97-115.

Biscaye P.E. (1965) Mineralogy and sedimentation of recent deep-sea clay in the Atlantic Ocean and adjacent seas and oceans. Geol. Soc. Am. Bull., 76, 803-832.

Boulesteix, K., Poyatos-Moré, M., Flint, S.S., Taylor, K.G., Hodgson, D.M., Hasiotis, S.T. (2019) Transport and deposition of mud in deep-water environments: Processes and stratigraphic implications. Sedimentology, doi: 10.1111/sed.12614.

Bouma, A.H. (1962) Sedimentology of some Flysch deposits; a graphic approach to facies interpretation, 168 pp. Elsevier, Amsterdam.

Carrapa, B., Di Giulio, A., Wijbrans, J. (2004). The early stages of the Alpine collision: an image derived from the Upper Eocene-Lower Oligocene record in the Alps-Apennines knot area. Sedimentary Geology, 171, 181-203.

Cavanna, F., Di Giulio, A., Galbiati, B., Mosna, S., Perotti, C.R., Pieri, M. (1989) Carta geologica dell'estremità orientale del Bacino Terziario Ligure-Piemontese [Translated title: Geological map of the western end of the Tertiary Ligure-Piemontese Basin]. Atti Ticinesi Scienze della Terra, 32.

Cibin, U., Di Giulio, A., Martelli L. (2003) Oligocene-Early Miocene evolution of the Northern Apennines (northwestern Italy) traced through provenance of piggy-back basin fill successions. In "Tracing tectonic deformation using the sedimentary record" (Eds. T. McCann and A. Saintot), Geol. Soc. London Spec. Pub., 208, 269-287.

Cibin, U., Di Giulio, A., Martelli, L., Catanzariti, R., Poccianti, S., Rosselli, C., Sani, F. (2004) Factors controlling foredeep turbidite deposition: the case of Northern Apennines (Oligocene-Miocene, Italy). In "Confined turbidite systems" (Eds. S. Lomas and P. Joseph), Geol. Soc. London Spec. Pub., 222, 115-134.

Di Giulio, A., Mancin, N., Martelli, L. (2002) Geohistory of the Ligurian orogenic wedge: first inferences from Epiligurian sediments. Boll. Soc. Geol. It, 121 special vol.1, 375-384.

Dorrell, R.M., Amy, L.A., Peakall, J. and McCaffrey, W.D. (2018) Particle Size Distribution Controls the Threshold Between Net Sediment Erosion and Deposition in Suspended Load Dominated Flows. Geophysical Research Letters, 45(3), 1443-1452.

Felletti, F. (2002) Complex bedding geometries and facies associations of the turbiditic fill of a confined basin in a transpressive setting (Castagnola Fm., Tertiary Piedmont Basin, NW Italy). Sedimentology, 49, 645-667.

Fonnesu, M., Patacci, M., Haughton, P.D.W., Felletti, F. and McCaffrey, W.D. (2016) Hybrid Event Beds Generated By Local Substrate Delamination On A Confined-Basin Floor. Journal of Sedimentary Research, 86(8), 929-943.

Fonnesu, M., Felletti, F., Haughton, P.D.W., Patacci, M. and McCaffrey, W.D. (2018) Hybrid event bed character and distribution linked to turbidite system sub-environments: The North Apennine Gottero Sandstone (north-west Italy). Sedimentology, 65(1), 151-190.

Gandolfi, G., Paganelli, L. and Zuffa, G.G. (1983) Petrology and dispersal pattern in the Marnoso-arenacea Formation (Miocene, Northern Apennines). Journal of Sedimentary Petrology, 53(2), 493-507.

Georgiopoulou, A., Wynn, R.B., Masson, D.G. and Frenz, M. (2009) Linked turbidite-debrite resulting from recent Sahara Slide headwall reactivation. Marine and Petroleum Geology, 26(10), 2021-2031.

Gladstone, C., Phillips, J.C. and Sparks, R.S.J. (1998) Experiments on bidisperse, constant-volume gravity currents; propagation and sediment deposition. Sedimentology, 45(5), 833-843.

Gutierrez-Pastor, J., Nelson, C.H., Goldfinger, C., Johnson, J E., Escutia, C., Eriksson, A.T. and Morey, A.E. (2009) Earthquake control of Holocene turbidite frequency confirmed by hemipelagic sedimentation chronology on the Cascadia and Northern California active continental margins. In: External Controls on Deep-Water Depositional Systems (Eds. Kneller, B.C., Martinsen, O.J. and McCaffrey, W.D.), Society for Sedimentary Geology Special Publication, 92, 179-197.

Haughton, P.D.W. (1994) Deposits of deflected and ponded turbidity currents, Sorbas Basin, Southeast Spain. Journal of Sedimentary Research, Section A: Sedimentary Petrology and Processes, 64(2), 233-246.

Haughton, P.D.W. (2000). Evolving turbidite systems on a deforming basin floor, Tabernas, SE Spain. Sedimentology, 47(3), 497-518.

Haughton, P.D.W., Davis, C., McCaffrey, W.D. and Barker, S. (2009). Hybrid sediment gravity flow deposits - Classification, origin and significance. Marine and Petroleum Geology, 26(10), 1900-1918.

Hovikoski, J., Therkelsen, J., Nielsen, L.H., Bojesen-Koefoed, J.A., Nytoft, H.P., Petersen, H.I., Abatzis, I., Tuan, H.A., Phuong, B.T.N., Dao, C.V. and Fyhn, M.B.W. (2016) Density-Flow Deposition In A Fresh-Water Lacustrine Rift Basin, Paleogene Bach Long Vi Graben, Vietnam. Journal of Sedimentary Research, 86(9), 982-1007.

Ibbeken, H., Schleyer, R. (1991) Source and Sediment. A Case Study of Provenance and Mass Balance at an Active Plate Margin (Calabria, Southern Italy). Springer, Berlin.

Ingersoll R.V., Bullard T.F., Ford R.L., Grimm J.P., Pickle J.D. and Sares S.W. (1984). The effect of grain size on detrital modes: a test of the Gazzi-Dickinson point-counting method. Journal of Sedimentary Petrology, 54, 103-116.

Ito, M. (2008). Downfan transformation from turbidity currents to debris flows at a channel-to-lobe transitional zone; the lower Pleistocene Otadai Formation, Boso Peninsula, Japan. Journal of Sedimentary Research, 78(10), 668-682.

Kane, I.A., Pontén, A.S.M., Vangdal, B., Eggenhuisen, J.T., Hodgson, D.M. and Spychala, Y.T. (2017). The stratigraphic record and processes of turbidity current transformation across deep-marine lobes. Sedimentology, 64(5), 1236-1273.

Liu, Q., Kneller, B., Fallgatter, C., Buso, V.V. and Milana, J.P. (2018) Tabularity of individual turbidite beds controlled by flow efficiency and degree of confinement. Sedimentology, 65(7), 2368-2387.

Lowe, D.R. (1988) Suspended-load fallout rate as an independent variable in the analysis of current structures. Sedimentology, 35(5), 765-776.

Macquaker, J.H.S., Bentley, S.J., Bohacs, K.M. (2010) Wave-enhanced sediment-gravity flows and mud dispersal across continental shelves: Reappraising sediment transport processes operating in ancient mudstone successions. Geology, 38(10), 947-950.

Maino, M., Decarlis, A., Felletti, F. and Seno S. (2013) Tectono-sedimentary evolution of the Tertiary Piedmont Basin (NW Italy) within the Oligo–Miocene central Mediterranean geodynamics. Tectonics, 32, 1-27.

Malgesini, G., Talling, P.J., Hogg, A.J., Armitage, D., Goater, A. and Felletti, F. (2015) Quantitative analysis of submarine-flow deposit shape in the Marnoso-Arenacea Formation: what is the signature of hindered settling from dense near-bed layers? Journal of Sedimentary Research, 85(2), 170-191.

Marini, M., Milli, S., Ravnas, R. and Moscatelli, M. (2015) A comparative study of confined vs semi-confined turbidite lobes from the Lower Messinian Laga Basin (Central Apennines, Italy): Implications for assessment of reservoir architecture. Marine and Petroleum Geology, 63, 142-165.

Marini, M., Patacci, M., Felletti, F. and McCaffrey, W.D. (2016A) Fill to spill stratigraphic evolution of a confined turbidite mini-basin succession, and its likely well bore expression: The Castagnola Fm, NW Italy. Marine and Petroleum Geology, 69, 94-111.

Marini, M., Felletti, F., Milli, S. and Patacci, M. (2016B) The thick-bedded tail of turbidite thickness distribution as a proxy for flow confinement: Examples from tertiary basins of central and northern Apennines (Italy). Sedimentary Geology, 341, 96-118.

Mehta, A.J. (2014) An Introduction to Hydraulics of Fine Sediment Transport. Advanced Series on Ocean Engineering, 38, 1060 pp.

Meiburg, E. and Kneller, B.C. (2010) Turbidity Currents and Their Deposits. Annual Review of Fluid Mechanics, 42, 135-156.

Moore D.M., Reynolds, R.C. (1989) X-ray Diffraction and the Identification and Analysis of Clay Minerals, 332 pp. Oxford University Press, New York.

Mosca, P., Polino, R., Rogledi, S., Rossi, M. (2010) New data for the kinematic interpretation of the Alps-Apennines junction (Northwestern Italy). International Journal of Earth Sciences, 99(4), 833-849.

Mueller, P., Patacci, M. and Di Giulio, A. (2017) Hybrid event beds in the proximal to distal extensive lobe domain of the coarse-grained and sand-rich Bordighera turbidite system (NW Italy). Marine and Petroleum Geology, 86, 908-931.

Mulder, T. and Alexander, J. (2001) The physical character of subaqueous sedimentary density flows and their deposits. Sedimentology, 48(2), 269-299.

Mutti, E. and Normark, W.R. (1987) Comparing examples of modern and ancient turbidite systems; problems and concepts. In: Marine clastic sedimentology; concepts and case studies (Eds. Leggett, J.K. and Zuffa, G.G.), p. 1-38. Graham and Trotman, London, United Kingdom.

Mutti, E., Tinterri, R., Remacha, E., Mavilla, N., Angella, S. and Fava, L. (1999) An Introduction to the Analysis of Ancient Turbidite Basins from an Outcrop Perspective. American Association of Petroleum Geologists, Tulsa, 61 p.

Mutti, E., Di Biase, D., Fava, L., Mavilla, N., Sgavetti, M. and Tinterri, R. (2002) The Tertiary Piedmont Basin. In: Revisiting turbidites of the Marnoso-arenacea Formation and their basin-margin equivalents: problems with classic models, Excursion Guidebook (Eds. Mutti, E., Ricci Lucchi, F. and Roveri, M.), pp. 1-25.

Patacci, M., Haughton, P.D.W. and McCaffrey, W.D. (2015) Flow Behavior of Ponded Turbidity Currents. Journal of Sedimentary Research, 85(8), 885-902.

Patacci, M. (2016) A high-precision Jacob's staff with improved spatial accuracy and laser sighting capability. Sedimentary Geology, 335, 66-69.

Pierce, C.S., Haughton, P.D.W., Shannon, P.M., Pulham, A.J., Barker, S.P. and Martinsen, O.J. (2018) Variable character and diverse origin of hybrid event beds in a sandy submarine fan system, Pennsylvanian Ross Sandstone Formation, western Ireland. Sedimentology, 65(3), 952-992.

Piper, D.J.W., Cochonat, P. and Morrison, M.L. (1999) The sequence of events around the epicentre of the 1929 Grand Banks earthquake; initiation of debris flows and turbidity current inferred from sidescan sonar. Sedimentology, 46(1), 79-97.

Porten, K.W., Kane, I.A., Warchol, M.J. and Southern, S.J. (2016) A Sedimentological Process-Based Approach To Depositional Reservoir Quality of Deep-Marine Sandstones: An Example From the Springar Formation, Northwestern Vøring Basin, Norwegian Sea. Journal of Sedimentary Research, 86(11), 1269-1286.

Rossi, M. and Craig, J. (2016) A new perspective on sequence stratigraphy of syn-orogenic basins: insights from the Tertiary Piedmont Basin (Italy) and implications for play concepts and reservoir heterogeneity. In: The Value of Outcrop Studies in Reducing Subsurface Uncertainty and Risk in Hydrocarbon Exploration and Production (Eds. Bowman, M., Smyth, H.R., Good, T.R., Passey, S.R., Hirst, J.P.P. and Jordan, C.J.), Geological Society of London Special Publication, 436, 93-133.

Sagri, M. (1979) Upper Cretaceous carbonate turbidites of the Alps and Apennines deposited below the calcite compensation level. Journal of Sedimentary Petrology, 49(1), 23-28

Southern, S.J., Patacci, M., Felletti, F. and McCaffrey, W.D. (2015) Influence of flow containment and substrate entrainment upon sandy hybrid event beds containing a co-genetic mud-clast-rich division. Sedimentary Geology, 321, 105-122.

Spychala, Y.T., Hodgson, D.M., Prelat, A., Kane, I.A., Flint, S.S. and Mountney, N.P. (2017) Frontal and Lateral Submarine Lobe Fringes: Comparing Sedimentary Facies, Architecture and Flow Processes. Journal of Sedimentary Research, 87(1), 75-96.

Sumner, E.J., Talling, P.J., Amy, L.A., Wynn, R.B., Stevenson, C.J. and Frenz, M. (2012) Facies architecture of individual basin-plain turbidites: Comparison with existing models and implications for flow processes. Sedimentology, 59(6), 1850-1887.

Talling, P.J., Malgesini, G., Sumner, E.J., Amy, L.A., Felletti, F., Blackbourn, G., Nutt, C., Wilcox, C., Harding, I.C. and Akbari, S. (2012) Planform geometry, stacking pattern, and extrabasinal origin of low strength and intermediate strength cohesive debris flow deposits in the Marnoso-arenacea Formation, Italy. Geosphere, 8(6), 1207-1230.

Talling, P.J. (2013) Hybrid submarine flows comprising turbidity current and cohesive debris flow: Deposits, theoretical and experimental analyses, and generalized models. Geosphere, 9(3), 460-488.

Talling, P.J. (2014) On the triggers, resulting flow types and frequencies of subaqueous sediment density flows in different settings. Marine Geology, 352, 155-182.

Talling, P.J., Allin, J., Armitage, D.A., Arnott, R.W.C., Cartigny, M.J.B., Clare, M.A., Felletti, F., Covault, J.A., Girardclos, S., Hansen, E., Hill, P.R., Hiscott, R.N., Hogg, A.J., Clarke, J.H., Jobe, Z.R., Malgesini, G., Mozzato, A., Naruse, H., Parkinson, S., Peel, F.J., Piper, D.J.W., Pope, E., Postma, G., Rowley, P., Sguazzini, A., Stevenson, C.J., Sumner, E.J., Sylvester, Z., Watts, C. and Xu, J.P. (2015) Key future directions for research on turbidity currents and their deposits. Journal of Sedimentary Research, 85(2), 153-169.

Tinterri, R. and Tagliaferri, A. (2015) The syntectonic evolution of foredeep turbidites related to basin segmentation: Facies response to the increase in tectonic confinement (Marnoso-arenacea Formation, Miocene, Northern Apennines, Italy). Marine and Petroleum Geology, 67, 81-110.

Tőkés L. and Patacci M. (2018) Quantifying tabularity of turbidite beds and its relationship to the inferred degree of basin confinement. Marine and Petroleum Geology, 97, 659-671.

Toniolo, H., Parker, G. and Voller, V. (2007) Role of ponded turbidity currents in reservoir trap efficiency. Journal of Hydraulic Engineering, 133(6), 579-595.

Van Andel, T.H. and Komar, P.D. (1969). Ponded sediments of the Mid-Atlantic Ridge between 22^{o} and 23^{o} north latitude. Geological Society of America Bulletin, 80(7), 1163-1190.

Weimer, P. and Slatt, R.M. (2007). Introduction to the Petroleum Geology of Deepwater Settings. AAPG Studies in Geology, 57, pp. 846.